Spectrometric Evidence for the Flavin−1-Phenylcyclopropylamine Inactivator Adduct with Monoamine Oxidase N†

Deanna J. Mitchell,‡ Dejan Nikolic,§ Edwin Rivera,|| Sergey O. Sablin,⊥ Sun Choi,‡ Richard B. van Breemen,§ Thomas P. Singer,⊥,# and Richard B. Silverman*,‡

Department of Chemistry and Department of Biochemistry, Molecular Biology, and Cell Biology, Northwestern University, Evanston, Illinois 60208-3113, Department of Medicinal Chemistry and Pharmacognosy, University of Illinois, Chicago, Illinois 60612-7231, Department of Medicinal Chemistry and Molecular Pharmacology, Purdue University, West Lafayette, Indiana 47907-1333, Department of Biochemistry and Biophysics, University of California, San Francisco, California 94121, and Molecular Biology Division, Department of , San Francisco, California 94121

Received February 23, 2001

ABSTRACT: 1-Phenylcyclopropylamine (1-PCPA) is shown to be an inactivator of the fungal flavoenzyme monoamine oxidase (MAO) N. Inactivation results in an increase in absorbance at 410 nm and is accompanied by the concomitant loss of the flavin absorption band at 458 nm. The spectral properties of the covalent adduct formed between the flavin cofactor of MAO N and 1-PCPA are similar to those reported for the irreversible inactivation product formed with 1-PCPA and mammalian mitochondrial monoamine oxidase B [Silverman, R. B., and Zieske, P. A. (1985) *Biochemistry 24,* 2128−2138]. There is a hypsochromic shift of the 410 nm band upon lowering the pH to 2, indicating that an N^5-flavin adduct formed upon inactivation. Use of the fungal enzyme, MAO N, which lacks the covalent attachment to the flavin adenine dinucleotide (FAD) cofactor present in the mammalian forms MAO A and MAO B, has allowed for the isolation and further structural identification of the flavin−inactivator adduct. The incorporation of two ^{13}C labels into the inactivator, [2,3-$^{13}C_2$]-1-PCPA, followed by analysis using on-line liquid chromatography/electrospray ionization mass spectrometry and nuclear magnetic resonance spectroscopy, provided a means to explore the structure of the flavin−inactivator adduct of MAO N. The spectral evidence supports covalent attachment of the 1-PCPA inactivator to the cofactor as *N*^{5}-3-oxo-3-phenylpropyl-FAD.

Monoamine oxidase (MAO; EC 1.4.3.4)[1] is a flavoenzyme responsible for the catalytic oxidative deamination of biogenic amines. MAO is known to degrade important neurotransmitters, such as serotonin, norepinephrine, and dopamine, as well as to oxidize benzylamine, phenylethylamine, and the tertiary amine 1-methyl-4-phenyl-1,2,3,6-tetrahydropyridine (MPTP) at significant rates (*1*, *2*). Therefore, the inhibition of this enzyme has been widely studied for application as a clinical treatment of neuropathological disorders such as Parkinson's disease and depression (*3*, *4*). Although monoamine oxidase has been studied for more than half a century, certain aspects of the enzyme, such as its substrate binding site and chemical mechanism, are still the focus of debate (*5*).

Mammalian monoamine oxidase exists as two isozymes: MAO A and MAO B (*6*). Both forms are homodimers, containing one covalently bound FAD cofactor per subunit (*7*). Recently another flavin-dependent monoamine oxidase, named MAO N, was isolated from the fungus *Aspergillus niger* (*8*, *9*). It has been reported that MAO N exhibits a similar substrate and inhibitor specificity and response to selective, irreversible inhibitors to those of MAO A and MAO B (*8*−*10*). This finding led to the proposal that MAO N is an evolutionary precursor of mammalian MAO A and MAO B (*10*). While a substantial portion of the amino acid sequence of the fungal enzyme resembles those of MAO A and MAO B, MAO N is a homotetramer, and lacks the covalent bond to the FAD cofactor (*8*, *9*). Sablin and coworkers have cloned, sequenced, expressed, and isolated pure MAO N (*10*), offering the possibility of studying the interaction and structure of inhibitors with the flavin cofactor without the complications that arise when the flavin is covalently attached to the enzyme (as with MAO A and MAO B). Lack of the attachment of the FAD cofactor to MAO N provides an avenue for acquiring structural data on flavin−inactivator adducts without the need for proteolytic digestion, purification of the peptide, or interference of amino acids.

† This work was supported by grants from the National Institutes of Health (Grant GM32634 to R.B.S. and Instrument Grant S10 RR10485 to R.B.v.B.).

* Correspondence should be addressed to this author at the Department of Chemistry, Northwestern University, Evanston, IL 60208-3113. Phone: (847) 491-5653, FAX: (847) 491-7713, E-mail: Agman@chem.nwu.edu.

‡ Northwestern University.

§ University of Illinois.

|| Purdue University.

⊥ University of California, San Francisco, and Veterans Affairs Medical Center.

Deceased June 16, 1999.

[1] Abbreviations: MAO, monoamine oxidase; LC/ESI-MS, liquid chromatography/electrospray ionization mass spectrometry; MS/MS, tandem mass spectrometry; 1-PCPA, 1-phenylcyclopropylamine; HMQC, heteronuclear correlation through multiple quantum coherence; ROESY, rotating frame nuclear Overhauser effect spectroscopy.

10.1021/bi010388q CCC: $20.00
Published on Web 04/05/2001

Scheme 1: Mechanism Proposed by Silverman and Zieske for the Inactivation of MAO B by 1-PCPA (*13*)

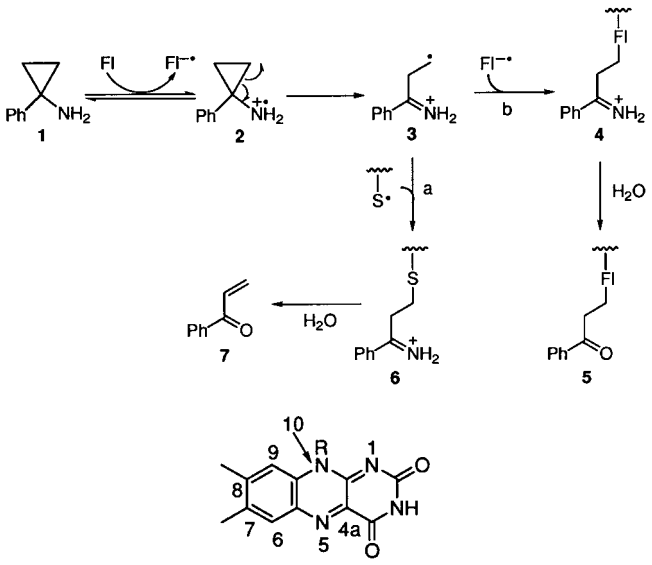

FIGURE 1: Structure and numbering system of the isoalloxazine ring of the oxidized flavin cofactor.

Cyclopropylamines are among the most extensively studied inactivators of mammalian MAO; *trans*-2-phenylcyclopropylamine is a current treatment for depression. Mechanistic studies have shown that some irreversible inactivators, such as *trans*-2-phenylcyclopropylamine, form a covalent attachment to an amino acid group in the enzyme (*11*, *12*). Another inactivator, 1-phenylcyclopropylamine (1-PCPA), forms two types of adducts with MAO B (*13*−*15*). One adduct is formed reversibly with a cysteine residue in MAO B (Scheme 1, pathway a), while the other is formed irreversibly by covalent attachment of the inactivator to the flavin cofactor (Scheme 1, pathway b). The mechanism proposed was a one-electron transfer from 1-PCPA (**1**) to the flavin, giving a flavin semiquinone (**2**), which is followed by homolytic cyclopropyl ring opening to a carbon radical intermediate (**3**). There are three positions on flavin cofactors that generally are modified by inactivators (Figure 1): the C^{4a}-position (*16*), the N^5-position (*17*), and the C^6-position (*18*), depending on the enzyme and inactivator. Combination of flavin semiquinone **2** with the 1-PCPA radical (**3**) was proposed to yield a stable N^5-flavin adduct (**5**); hydrogen atom transfer from a cysteine residue to the flavin semiquinone to give the cysteine radical, followed by reaction with **3**, produces the cysteine adduct (**6**), which spontaneously decomposes to acrylophenone (**7**). Pathway a predominated over pathway b by a factor of 7. Evidence for the formation of a cysteine adduct comes from a related study using *N*-cyclopropyl-α-methylbenzylamine (**8**), which also

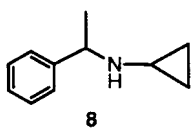

was shown to inactivate MAO B, but only by attachment to an active site amino acid residue, not to the flavin cofactor (*19*). This adduct was stabilized by sodium borohydride reduction; then proteolysis, HPLC, and mass spectrometry provided evidence for the adduct structure and showed the attachment of the inactivator to be to Cys-365. Evidence for the formation of a flavin adduct by inactivation of MAO B by 1-PCPA comes from experiments with radioactively labeled inactivator (*13*). A 1:1 stoichiometry of radioactivity to the active site was observed, and the flavin spectrum was reduced, even under denaturing conditions. However, because the flavin in MAO B is covalently bound to the protein, a more positive identification of the flavin adduct was impractical. The flavin adduct would have been much more easily identified if the flavin were not covalently bound. MAO N provides that option.

In this paper, we report the isolation of the 1-PCPA−flavin adduct of MAO N by reversed-phase high-performance liquid chromatography (RP-HPLC) and subsequent assignment of its structure using UV−vis spectroscopy, liquid chromatography/electrospray ionization mass spectrometry (LC/ESI-MS), and NMR spectrometry. In light of the similarity of MAO N to mammalian MAO A and MAO B (*8*−*10*), the structural analysis of this inactivation product also offers insight into the corresponding structure of the adduct with the mammalian MAOs.

EXPERIMENTAL PROCEDURES

Materials. All materials were of the highest grade available from Aldrich Chemical Co., Sigma Chemical Co., or Calbiochem. HPLC solvents were purchased from Fisher Scientific and filtered through Gelman 0.45 μm membranes. Centricon-30 microconcentrator tubes were purchased from Amicon. The 3 mm NMR tube was purchased from Shigemi, Inc. Deuterium oxide, Ultra-D, 99.999 atom % D, was purchased from Isotech, Inc. 1-PCPA and [2,3-$^{13}C_2$]-1-PCPA were synthesized as previously reported (*13*, *20*).

Analytical Methods. Enzyme purification was carried out as previously reported (*10*). MAO N assays and UV−vis spectra were recorded on a Perkin-Elmer Lambda 10 spectrophotometer. Measurements of pH were performed on an Orion 701-A pH meter equipped with a general combination electrode. Low molecular weight impurities were removed using Pharmacia Biotech PD-10 columns (Sephadex 25 M). A Du Pont Sorvall RC5B Plus centrifuge was used with an SLA-600 rotor for centrifugations. Amicon Centricon-30 microconcentrator tubes, prewashed with doubly distilled water, were used for sample concentration. An Eppendorf Microfuge, model 5415C, was used for microcentrifugations. Ultrasonication was accomplished using a cavitator ultrasonic cleaner from Mettler Electronics Corp. Lyophilization was accomplished using a Heto CT60e lyophilizer. A Savant SC100 speed vac concentrator, equipped with a Savant RT 100 refrigerated condensation trap, was used to dry the samples. HPLC was performed on a Beckman 125P solvent delivery module, equipped with a Beckman 166 detector and Nouveau Gold software. Injections were monitored at 410 nm, unless otherwise specified. The HPLC system was equipped with a 250 × 4.6 mm Alltech Alltima C18, 100 Å, 10 μm, analytical column. The LC system coupled to the mass spectrometer consisted of an ABS 140A syringe pump, a Rheodyne injector model 7725 equipped with a 10 μL injection loop, and a 2 × 250 mm, 5 μm, Hewlett-Packard Hypersil BDS C18 column. Electrospray ionization mass spectra were acquired using a Micromass Quattro II mass spectrometer (Fisons Instruments, Manches-

ter, U.K.). NMR spectra were recorded on a Varian Unity Plus 600 MHz spectrometer equipped with a Nalorac 3 mm probe. A 3 mm Shigemi NMR tube, 80 μL volume, was used for NMR measurements. Molecular modeling was performed using the Sybyl program, software version 6.6.

Enzyme and Assays. MAO N growth and purification were performed by Sablin and co-workers as reported (*10*). Spectrophotometric assays were carried out in 50 mM Tris buffer, pH 7.2. Benzylamine (10 mM) was the substrate, and the scan range was 200−600 nm. Protein concentrations were measured using a modified Bradford procedure (*21*) and the Bio-Rad Protein Reagent. Determination of the concentration of active MAO N was based on the difference in absorbance between oxidized (before benzylamine was added) and reduced (after benzylamine was added) enzyme at 458 nm. The extinction coefficient for MAO N at 458 nm is 10.7 $mM^{-1}cm^{-1}$ (*10*).

Oxidation and Inactivation of MAO N. The MAO N enzyme (3 mL, 186 μM) was divided evenly into two vials. To each vial was added potassium ferricyanide (25 μL, 1 M solution). The enzyme was incubated on ice for 25 min, and then applied to a PD-10 column, equilibrated with Tris buffer, 50 mM, pH 7.2. The enzyme was eluted with Tris buffer. The total volume of enzyme (10.5 mL) was divided (3 vials, 3.5 mL each). To each vial was added 1-PCPA, to a final concentration of 5 mM. The enzyme and inactivator were incubated at 4 °C for 14 h.

The above procedure was repeated, replacing 1-PCPA with the labeled inactivator [2,3-$^{13}C_2$]-1-PCPA. The final concentration of [2,3-$^{13}C_2$]-1-PCPA was 9 mM.

1-PCPA and [2,3-$^{13}C_2$]-1-PCPA Adduct Isolation. After complete inactivation, excess inactivator was removed using prerinsed Centricon-30 tubes, followed by a PD-10 column (enzyme eluted with water). The enzyme was denatured and precipitated by adding cold acetone to enzyme in cold water, 1:1, and incubating on ice (30 min). The cloudy solution was then sonicated (5 min), and microfuged [14 000 rpm (16000*g*), 15 min]. The yellow supernatant was collected and dried by speed vac to yield an orange solid. The solid was stored at −80 °C.

RP-HPLC and UV−Vis Analysis of the 1-PCPA and [2,3-$^{13}C_2$]-1-PCPA Adducts. The orange solid was dissolved in approximately 500 μL of water. An aliquot of ∼50 μL was set aside for LC/ESI-MS. Three separate aliquots (150 μL each) were injected onto the Alltech Alltima C18 column (4.6 × 250 mm, 10 μm) and eluted using the following system: mobile phase A, 95:5 water/acetonitrile (v/v); mobile phase B, 95:5 (v/v) acetonitrile/water; gradient, 5% B to 50% B over 20 min; at 24 min, return to 5% B over 2 min (except for the results in Figure 12, which were obtained with a gradient of 5% B to 40% B over 20 min). The flow rate was 1.0 mL/min. The visible range tungsten lamp detector was set at 410 nm. Under these conditions, unreacted flavin was observed to elute at 2−3 min and the modified flavin at 7−7.5 min. The collected fractions were subjected to UV−vis spectroscopy, scan range 250−600 nm, then dried by speed vac, and stored at −80 °C.

Electrospray Ionization Mass Spectrometry of the 1-PCPA and [2,3-$^{13}C_2$]-1-PCPA Adducts. The adducts were isolated as described above. The aliquot that was not subjected to RP-HPLC purification was diluted with water and used for mass spectral analysis. Aliquots of 5 μL each were loop-injected onto a Hypersil BDS C18 column (2 × 250 mm, 5 μm), connected to the mass spectrometer. The adduct was eluted with the following system: mobile phase A, 95:5 water/acetonitrile (v/v); mobile phase B, 95:5 (v/v) acetonitrile/water; gradient, 5% B to 40% B or 5% B to 50% B over 20 min. The flow rate was 0.190 mL/min. There was no split or postcolumn addition. Negative ion mode electrospray ionization (ESI^-) mass spectra were acquired. Instrument tuning parameters (ESI^-) were used along with the following operational parameters: capillary 2.90 kV; cone voltage 45 V; and source temperature 140 °C. The mass range was set at 420−970 amu, with a scan rate of 2 s/scan. Tandem mass spectra with a scan range of 100−600 amu were acquired with a collision energy of 26 eV and argon gas pressure of 3×10^{-3} mbar.

NMR Studies of the [2,3-$^{13}C_2$]-1-PCPA Adduct. Deuterium oxide (99.999 atom % D) was used for all operations. The 3 mm Varian Shigemi tube was prewashed with deuterium oxide and lyophilized. The HPLC-purified orange solid was dissolved in 100 μL of deuterium oxide and dried by speed vac (3 times) to minimize the presence of water. The dried sample was then dissolved in 40 μL of deuterium oxide and loaded into the NMR tube. The Eppendorf that contained the adduct was washed successively with 20 μL quantities of deuterium oxide (2 times) and added to the NMR tube for a final volume of 80 μL. The ^{1}H chemical shifts were referenced with respect to DSS (^{1}H, $\delta = 0$ ppm) at 25 °C.

All NMR experiments for the adduct were performed on a Varian Unity Plus 600 MHz NMR instrument, except the experiments with intact FAD, which were performed on an INOVA 500 MHz NMR instrument. The experiments were performed with a 3 mm inverse detection probe with pulse field gradients from Nalorac. ^{1}H-^{13}C correlations were determined via standard 1D ^{1}H-^{13}C heteronuclear multiple quantum coherence (HMQC) experiments (*22*) with the following acquisition parameters: sw(^{1}H) = 10 000 Hz; sw(^{13}C) = 45 243.7 Hz; pw(^{1}H, 90) = 5.4 μs at 63 dB ∼50 W; pw(^{13}C, 90) = 15 μs at 60 dB ∼300 W; $(\gamma B_1)/2 = 2$ kHz; and $T = 25$ °C.

RESULTS

Inactivation of MAO N and Absorption Spectra. FAD in MAO N exists partially in the semiquinone form, which is oxidized by treating the enzyme with a solution of potassium ferricyanide. This activates the enzyme and results in a decrease in the intensity of the absorption band at 380 nm and an increase in the band at 446 nm. Incubation of MAO N with 1-PCPA at 30 °C leads to a rapid loss of enzyme activity. With 1 mM of the 1-PCPA inhibitor, 50% of the enzyme activity is lost in 4 min; with 2 mM 1-PCPA, 50% activity is lost in 3 min. The inactivation of MAO N by 1-PCPA and by [2,3-$^{13}C_2$]-1-PCPA was monitored by UV−vis spectroscopy. Bleaching of the flavin band at 456 nm was accompanied by a simultaneous appearance of a new peak at 410 nm (Figure 2). When the absorption spectrum of the modified flavin was taken at pH 2.0, a red shift occurs relative to the spectrum at pH 7.2 (Figure 3).

LC/ESI-MS Characterization of the Flavin Adduct. The total ion chromatogram of the flavins from MAO N incubated

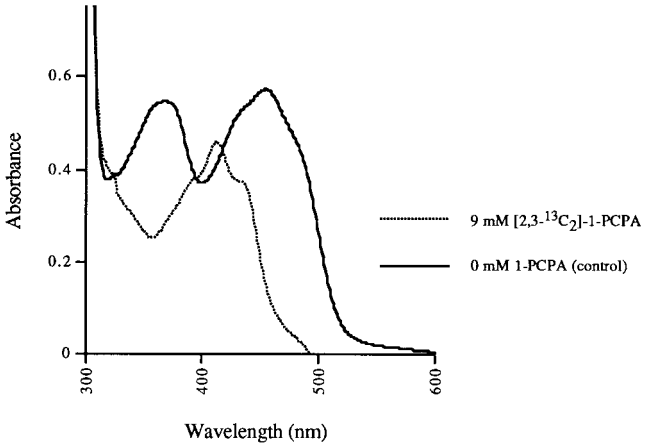

FIGURE 2: UV−vis spectra of MAO N with 0 mM 1-PCPA (control) and 9 mM [2,3-$^{13}C_2$]-1-PCPA, after incubation at 4 °C, 14 h.

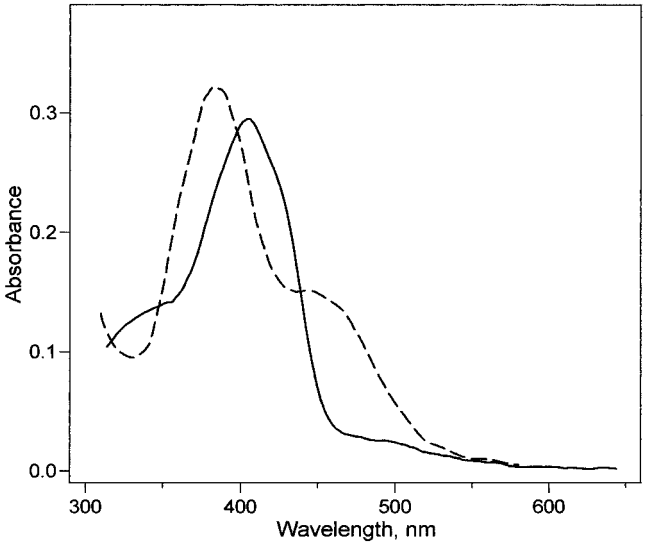

FIGURE 3: UV−vis spectra at pH 7.2 (solid line) and pH 2.0 (dashed line) of MAO N inactivated by 1-PCPA.

with 1-PCPA is shown in Figure 4. Four major products were detected. The mass spectra for the peaks at 8.8 min (Figure 5), 11.9 min (Figure 6), 14.2 min (Figure 7), and 14.4 min (Figure 8) are given with consistent structures for these masses adjacent to them. The total ion chromatogram of the flavins from MAO N incubated with [2,3-$^{13}C_2$]-1-PCPA is shown in Figure 9. The two peaks at about 2−2.3 min were identified as FAD and FMN. The mass spectra for the peaks at 6.6 and 7.0 min are shown in Figures 10 and 11, respectively. Five hours after the flavins from the [2,3-$^{13}C_2$]-1-PCPA-inactivated MAO N were isolated, the total ion chromatogram was recorded (Figure 12). The elution solvent was changed to spread out the peaks (see Experimental Procedures), but the two peaks formerly found at 6.6 and 7.0 min had become just one peak at 8.9 min. The mass spectrum of that new peak was the same as that of each of the original peaks (Figures 10 and 11).

NMR Studies on the [2,3-$^{13}C_2$]-1-PCPA Adduct. Figure 13 compares the 1D proton spectrum of unmodified FAD (spectrum b) to the ^{13}C-labeled FAD adduct resulting from the inactivation of MAO N by [2,3-$^{13}C_2$]-1-PCPA (spectrum a). The 1D HMQC-decoupled spectrum of the labeled adduct is shown in Figure 14.

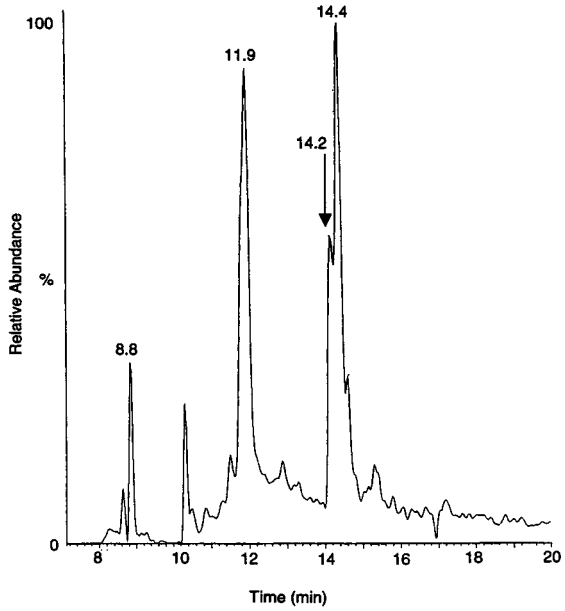

FIGURE 4: Total ion chromatogram of MAO N inactivated with 9 mM 1-PCPA.

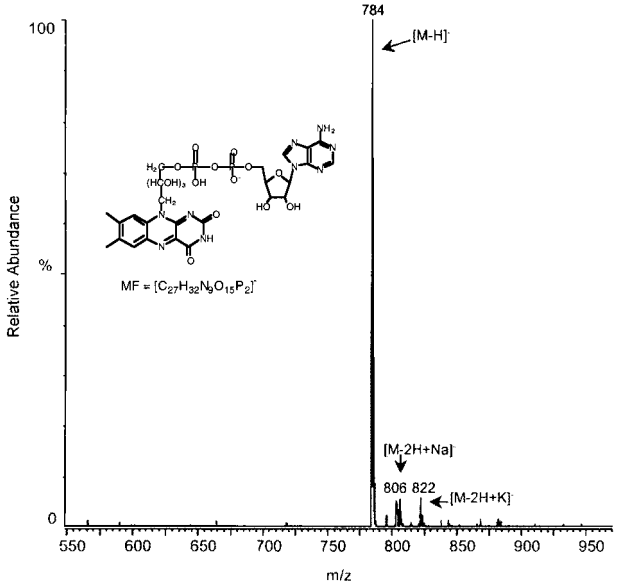

FIGURE 5: Negative mode electrospray ionization mass spectrum of the peak in the TIC with a retention time of 8.8 min from the incubation of MAO N with 9 mM 1-PCPA.

DISCUSSION

UV−vis analysis of the MAO N after purification indicated that the enzyme contained approximately 10−40% of the flavin cofactor in the semiquinone form (*10*). To ensure maximum enzyme activity, the FAD in the semiquinone form was oxidized by treating the enzyme with a solution of potassium ferricyanide.

Incubation of MAO N with 1-PCPA at 30 °C led to a rapid loss of enzyme activity. In light of the finding that MAO N shares a striking similarity to MAO A and MAO B in the N-terminal $\beta\alpha\beta$-fold consensus domain that binds the ADP moiety of FAD (*9*) and that it also oxidizes typical substrates for these enzymes (*10*), it is not surprising that 1-PCPA, a known mechanism-based inactivator of MAO B (*13*), also inactivates MAO N. The inactivations of MAO N by 1-PCPA and by [2,3-$^{13}C_2$]-1-PCPA were monitored by

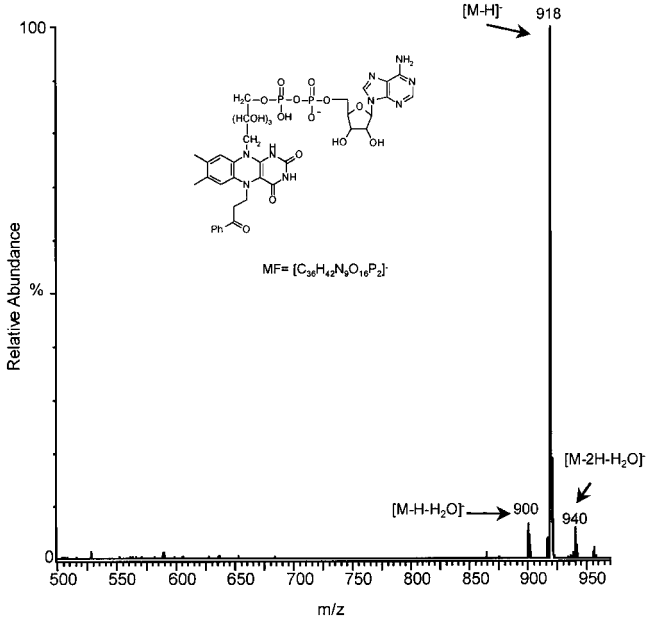

FIGURE 6: Negative mode electrospray ionization mass spectrum of the peak with a retention time of 11.9 min from the incubation of MAO N with 9 mM 1-PCPA.

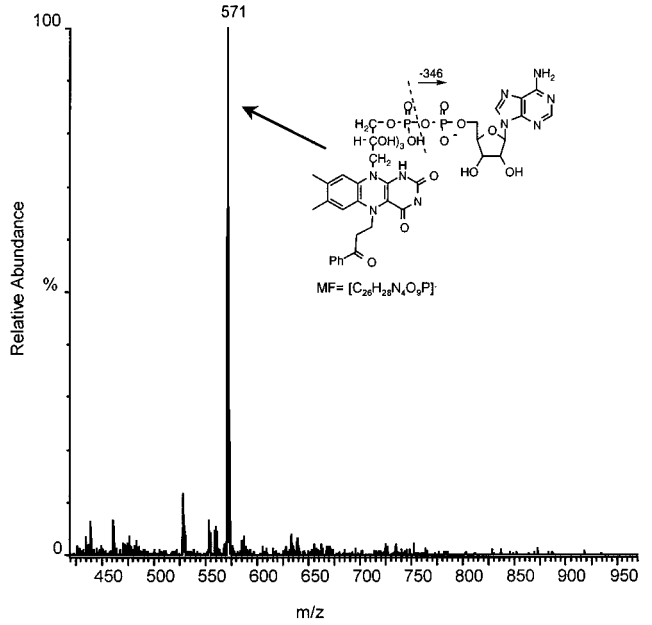

FIGURE 7: Negative mode electrospray ionization mass spectrum of the peak with a retention time of 14.2 min from the incubation of MAO N with 9 mM 1-PCPA.

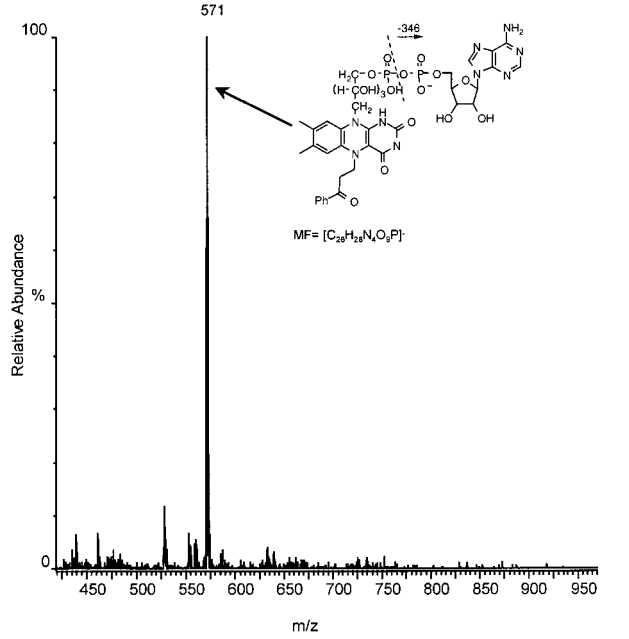

FIGURE 8: Negative mode electrospray ionization mass spectrum of the peak with a retention time of 14.4 min from the incubation of MAO N with 9 mM 1-PCPA.

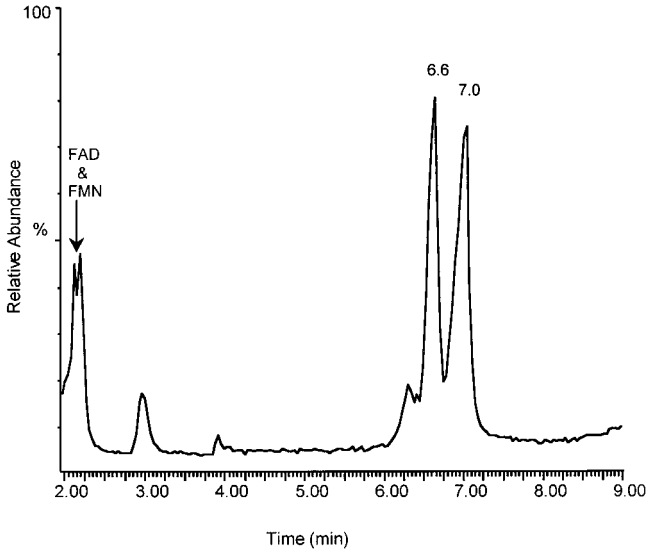

FIGURE 9: Initial total ion chromatogram of MAO N incubated with 9 mM [2,3-$^{13}C_2$]-1-PCPA.

UV−vis spectroscopy. Bleaching of the band of the flavin at 456 nm was accompanied by the simultaneous appearance of a new peak at 410 nm (Figure 2). The disappearance of the 456 nm band was evidence that modification of the flavin accompanied inactivation. Upon adjusting the pH from 7.2 to 2.0, the adduct absorbance band at 410 nm shifted hypsochromically (Figure 3). Whereas C^{4a}-flavin adducts exhibit a bathochromic shift under acidic conditions, the hypsochromic shift has been shown to be characteristic of N^5-flavin adducts (*23*). Similar observations have resulted from the reaction of MAO N with deprenyl and clorgyline, which have been proposed to form adducts with the flavin via a covalent attachment to the N^5-position (*10*). The UV−vis shift of the MAO N adduct under acidic conditions coupled with the stability of the adduct to several deproteinization agents support an N^5-attachment of the 1-PCPA inactivator to the flavin.

With MAO B, 1-PCPA inactivates by forming two products: a reversible product with an active site cysteine residue and an irreversible product with the flavin cofactor in a ratio of 1:7 (Scheme 1) (*13*, *14*). With MAO N, this partitioning of products does not appear to be occurring. Spectral changes exactly follow the loss of activity, indicating that modification of the flavin accompanies enzyme inactivation.

Structural studies of the adduct continued with on-line electrospray ionization mass spectrometry (LC/ESI-MS). The phosphate groups present on the FAD cofactor make it highly amenable to negative mode electrospray ionization. Acquisition of mass spectra of commercially available unmodified FAD allowed for the optimization of both liquid chroma-

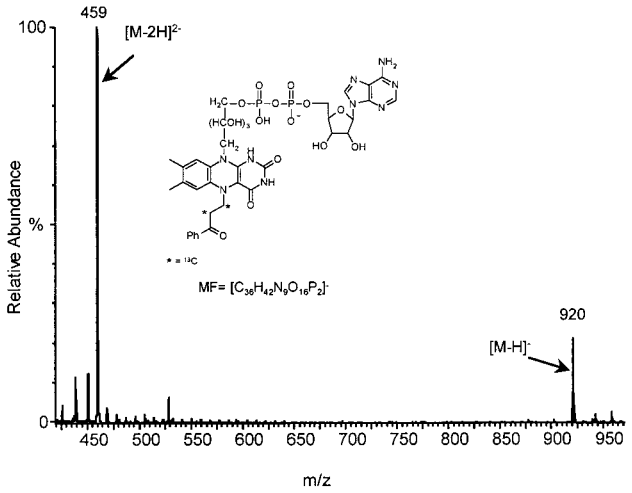

FIGURE 10: Negative mode electrospray ionization mass spectrum of the peak with a retention time of 6.6 min from the incubation of MAO N with 9 mM [2,3-$^{13}C_2$]-1-PCPA.

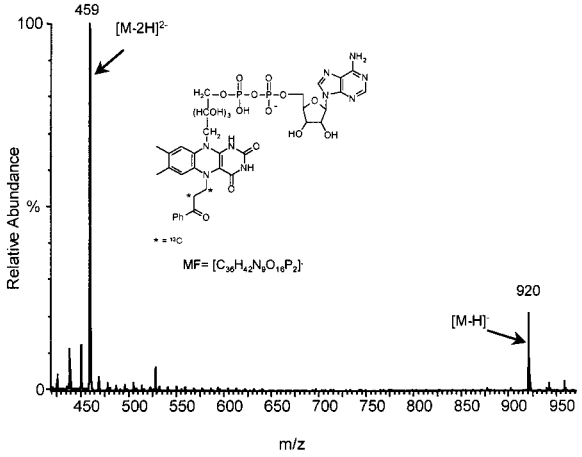

FIGURE 11: Negative mode electrospray ionization mass spectrum of the peak with a retention time of 7.0 min from the incubation of MAO N with 9 mM [2,3-$^{13}C_2$]-1-PCPA.

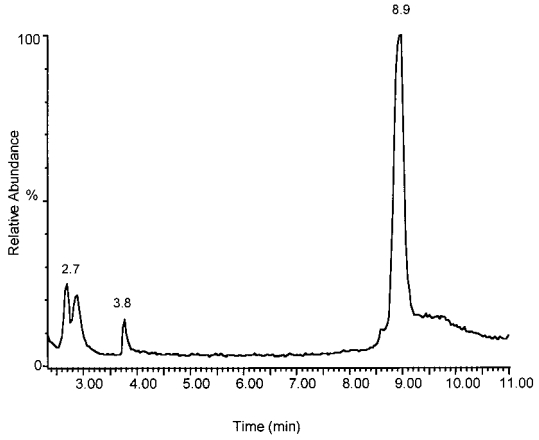

FIGURE 12: Total ion chromatogram of MAO N incubated with 9 mM [2,3-$^{13}C_2$]-1-PCPA after 5 h at 25 °C.

tography and mass spectrometry parameters. An injection of the adduct resulting from the inactivation of MAO N with 1-PCPA yielded several identifiable peaks in the total ion chromatogram (Figure 4). The peak present at 8.8 min was identified as unmodified FAD with a *m*/*z* of 784 (Figure 5). The presence of unmodified FAD was most likely the result of either incomplete inactivation by MAO N or adduct

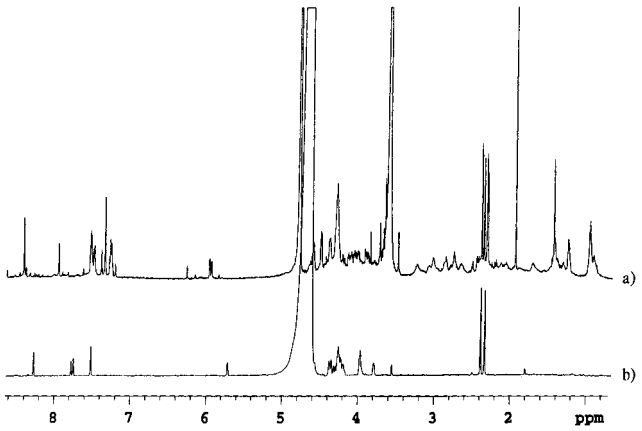

FIGURE 13: (a) Coupled proton NMR spectrum of the flavin adduct formed when MAO N is inactivated by [2,3-$^{13}C_2$]-1-PCPA and (b) coupled proton NMR spectrum of FAD.

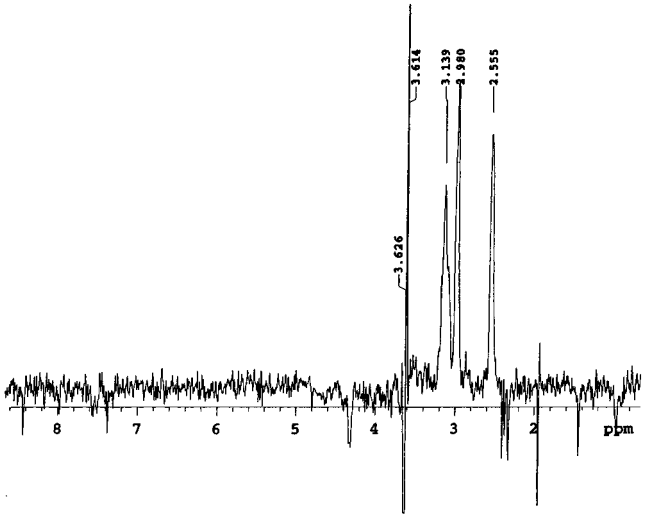

FIGURE 14: 1D HMQC decoupled spectrum of the flavin adduct formed when MAO N is inactivated by [2,3-$^{13}C_2$]-1-PCPA.

decomposition (vide infra). The peak with a retention time of 11.9 min corresponds to a 1-PCPA-modified FAD (*m*/*z* 918, Figure 6); a structure consistent with this mass is given on the spectrum. This is the structure that was proposed earlier based on radioactively labeled inactivator studies (*13*). MS/MS of the *m*/*z* 918 peak and multiple reaction monitoring (MRM) of the transitions *m*/*z* 918 to 346 and *m*/*z* 918 to 571 both confirmed that the *m*/*z* 918 peak was a modified form of FAD (data not shown). Fragmentation of the mass at *m*/*z* 918 gave a peak at *m*/*z* 346, which corresponds to AMP and is similar to FAD fragmentation.

Two peaks with retention times of 14.2 and 14.4 min, both with a *m*/*z* of 571, were also present (Figures 7 and 8, respectively). Because a mass of 571 is the result of the modified FAD (918) minus AMP (346) and a proton for negative mode ionization, these peaks correspond to a modified FMN. They are not the result of fragmentation of the modified FAD product and loss of AMP in the electrospray source because they are observed as distinct chromatography peaks. The fact that the two peaks have the same exact mass is suggestive of two isomers. Presumably, the corresponding FAD isomers coelute at 11.9 min (note that the 11.9 min peak is not symmetrical).

To confirm that the peaks with *m*/*z* of 918 are, in fact, derived from flavin−1-PCPA adducts, the correspond-

Scheme 2: Difference in the Decomposition of the C^{4a}- and N^5-Flavin−1-PCPA Adducts

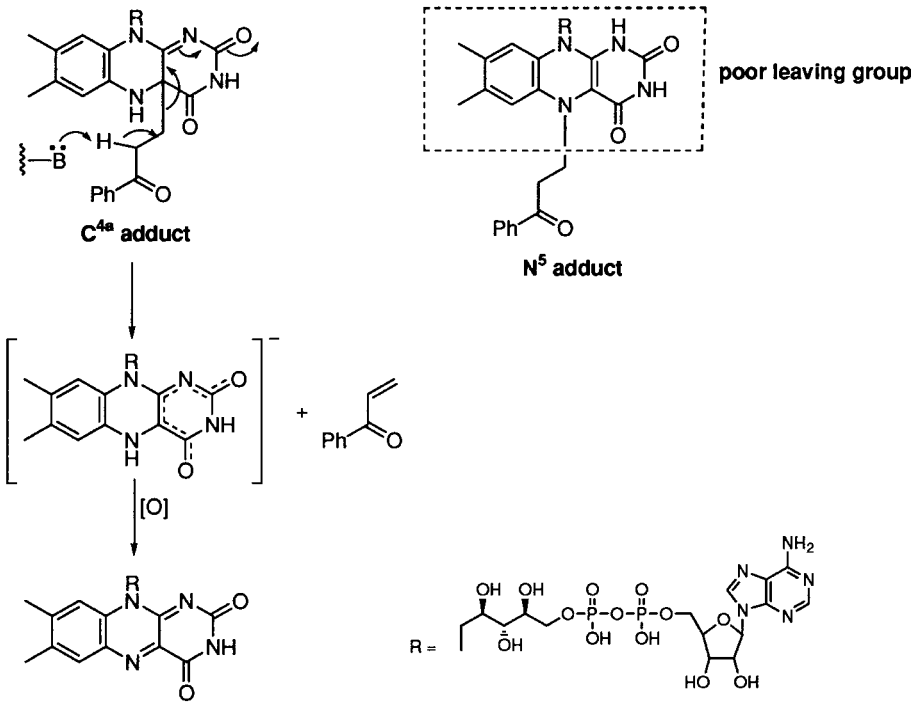

ing ^{13}C-labeled inactivator, [2,3-$^{13}C_2$]-1-PCPA, was synthesized; inactivation with this analogue should give a peak with a *m*/*z* of 920. The sample was subjected to the same LC and ESI-MS conditions as the unlabeled sample. Slight changes in the retention times of the identified peaks were attributed to minor changes in the mobile phase composition, incomplete equilibration of the column, and an alteration in the gradient used to elute the adduct. The initial injection of the [2,3-$^{13}C_2$]-1-PCPA adduct yielded four main peaks in the TIC (Figure 9). The two peaks present at 2.1 and 2.2 min were identified as unmodified FAD (*m*/*z* 784) and FMN (*m*/*z* 455), respectively. The two peaks in the TIC at 6.6 and 7.0 min have identical *m*/*z* (Figures 10 and 11) of 920, 2 amu higher than the unlabeled inactivator adduct, as expected for the two ^{13}C atoms. Once again, it appears that there are two isomers that form from the inactivation. After 5 h at room temperature, however, a second injection of the same sample yielded the peaks in the TIC (Figure 12) corresponding to FAD (2.7 min, *m*/*z* 784; the 2.9 min peak is a contaminant) and FMN (3.8 min, *m*/*z* 455), but only a single peak (at 8.9 min) with a *m*/*z* value of 920 (spectrum not shown). Retention times were lengthened by approximately 2 min from the earlier injection as the result of a modification to the LC gradient. The gradient was slowed (5% B to 40% B over 20 min) to spread out the peaks and ensure that the two isomers observed initially had collapsed to one isomer and not simply coeluted.

A tandem MS/MS experiment was performed to demonstrate that the two ^{13}C labels were incorporated on the isoalloxazine ring. Daughters of the *m*/*z* 920 peak showed two main fragments: *m*/*z* 346, corresponding to AMP, and *m*/*z* 573, corresponding to the isoalloxazine ring with the labeled adduct bound. The MS/MS spectrum of the unlabeled 1-PCPA adduct showed mass fragments of *m*/*z* 346 (AMP) and *m*/*z* 571, 2 amu lower than the daughter from the [2,3-$^{13}C_2$]-1-PCPA adduct.

NMR spectrometry also indicated that the inactivator becomes attached to the flavin at the N^5-position. A coupled proton NMR spectrum of the sample was acquired (Figure 13a). Several new peaks appeared which were not present in the NMR spectrum of unmodified FAD (Figure 13b), most apparent in the regions of 2−4 and 7−9 ppm. Assignment of resonances in the unmodified FAD was reported (*24*), and aided in the assignment of the resonances in the FAD−1-PCPA adduct. The HMQC experiment employs inverse detection to gain information about the correlation between ^{13}C and the directly attached ^1H (J_1CH) (*22*). The 1D HMQC decoupled spectrum is shown in Figure 14. The peak with a chemical shift of 3.6 ppm is an impurity, most likely introduced during sample isolation. There are new proton peaks in the region 2.56−3.14 ppm, more indicative of protons on a carbon adjacent to a nitrogen atom (such as the N^5-position of flavin) than protons on a carbon adjacent to another carbon atom (such as the C^{4a}-position of flavin). The additional aromatic protons also support the structure of the proposed flavin−1-PCPA adduct.

There are several possible explanations to account for the observations by mass spectrometry that more than one isomeric product results from the inactivation of MAO N by 1-PCPA; the two more likely possibilities are the following:

(1) Two confomers, both N^5 adducts, form initially. If one of the two confomers is a lower energy conformation, then after several hours at room temperature only the thermodynamic product would exist in solution, and only one peak would appear in the total ion chromatogram (as was observed in Figure 12).

(2) Two adducts, one at the C^{4a}-position and the other at the N^5-position, form initially. Because 1-PCPA bound at the C^{4a}-position is a better leaving group, it is less stable than the N^5 adduct (Scheme 2); therefore, it could decompose more rapidly, leaving only the N^5 adduct.

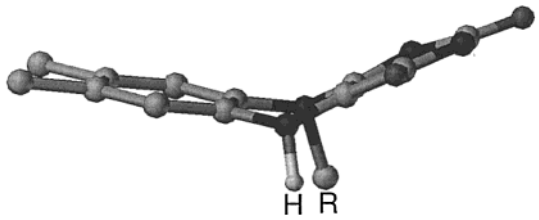

FIGURE 15: Molecular model of reduced lumiflavin.

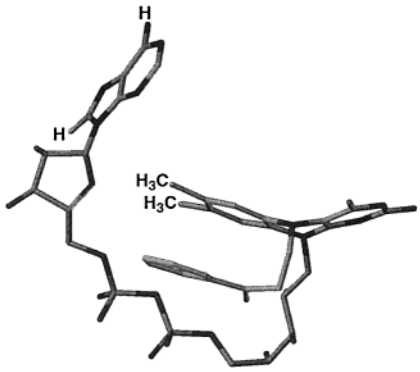

FIGURE 16: Energy-minimized molecular model of FAD with 1-PCPA bound at the N^5-position.

Two conformers are possible because reduced flavins are not planar; they bend along the N^5-N^{10} axis to yield a bent or "butterfly" shape (Figure 15) (*25*−*29*). Ab initio molecular orbital theory suggests the bent shape of the reduced flavin has a ring puckering angle of 27.3° along the N^5-N^{10} axis (*29*). The nonplanarity of the reduced flavin has been attributed to both electron repulsion and steric effects. In contrast to the theoretical data, NMR studies usually show the reduced flavin ring as planar, most likely because the barrier to the interconversion of the two bent structures is low, less than 20 kJ/mol (4.8 kcal/mol) (*26, 27*), and NMR studies are unable to distinguish between a single planar structure or two bent structures in fast equilibrium (*29*). In lumiflavin, the N^5 and N^{10} centers are a hybrid between sp^2 and sp^3, less pyramidal than tetrahedral, with the N^5 methyl and N^{10} proton pointing in opposite directions (*29*). One of the two butterfly conformations could be more stable than the other, depending upon the orientation of the sterically bulky substituents attached to the N^5 and N^{10} centers. With 1-PCPA bound to FAD (Figure 16), hydrophobic interactions (π-stacking) between the inactivator aromatic ring and the flavin aromatic ring could help to stabilize one of the conformations. The aromatic ring of the ADP also could undergo a π-stacking interaction with the flavin aromatic ring. Although the α-carbons of the substituents at the N^5- and N^{10}-positions of the FAD−1-PCPA adduct are methylenes, the addition of the sterically bulky 1-PCPA inactivator at N^5 and the ADP group of FAD at N^{10} could raise the barrier of interconversion between the bent forms, which involves both a ring flattening and nitrogen inversion, and could allow for the initial isolation of the two conformers.

Support for the π-stacked conformation depicted in the energy-minimized model shown in Figure 16 comes from NMR studies. A weak nuclear Overhauser effect between the C^2 and C^8 protons on the adenosine ring and the methyl protons on the isoalloxazine ring was observed (Figure 17), indicating a flexibility in the chain attached to the N^{10}-position and the potential for stacking interactions, depending upon the orientation of the adduct at N^5. Steric effects, such as substitution at N^5, have been shown by previous NMR studies to govern the conformation of reduced flavin (*27*). Two isomeric flavin adducts could result from the reaction of the planar semiquinone flavin with the cyclopropyl ring-opened radical species; once the reduced flavin is released from the enzyme, it could gradually overcome the inversion barrier, leading to the more stable isomer.

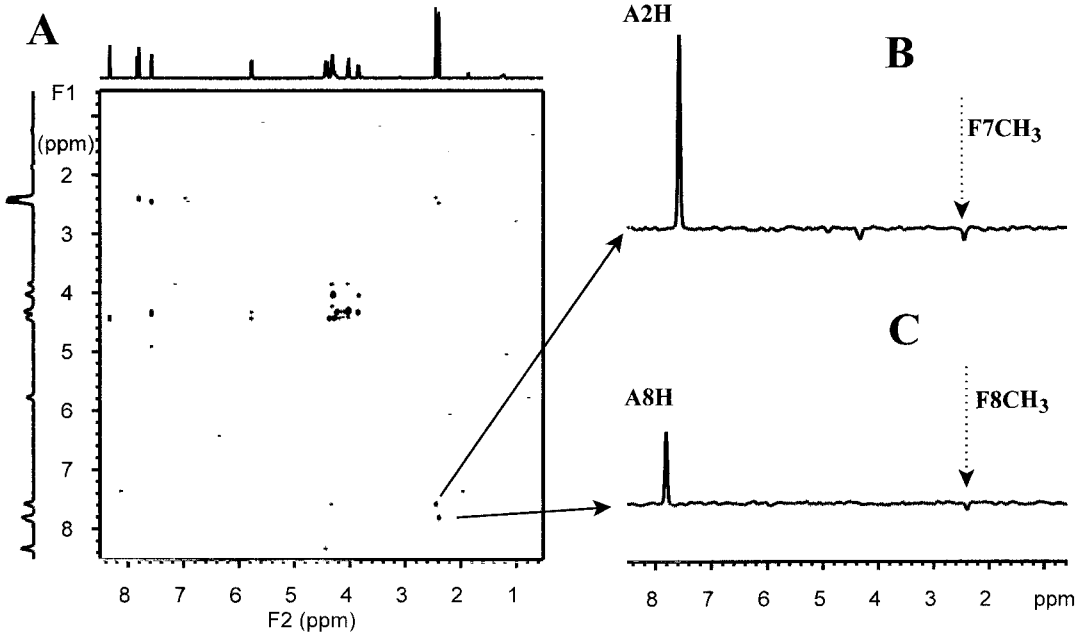

FIGURE 17: ROESY spectrum of FAD (120 μM concentration) in D_2O. 500 MHz proton ROESY NMR spectrum (mixing time 400 ms) of 120 μM FAD at 298 K in D_2O, pH 7.4. (A) 2D plot showing only ROESY cross-peaks (negative peaks) for clarity; diagonal peaks (positive) not shown. (B) 1D trace showing the adenine C^2 proton diagonal peak (positive) (A2H) and the flavin C^7 methyl cross-peak (negative) ($F7CH_3$). Also shown is a cross-peak between the adenine C^2 proton (A2H) and the ribose ring (at 4.4 ppm). (C) 1D trace showing the adenine C^8 proton diagonal peak (positive) (A8H) and the flavin C^8 methyl cross-peak (negative) ($F8CH_3$) of FAD.

Conformers, however, are usually interconverted so rapidly that they cannot be isolated as individual species, although conformational isomers with barriers on the order of 20−25 kcal/mol have been separated and characterized (*30*). While it is difficult to assign a value to the interconversion barrier of the FAD−1-PCPA adduct, comparison to the binding energy associated with aromatic nucleobases and DNA intercalators seems appropriate. The major stabilizing forces that contribute to the integrity of duplex DNA and RNA are noncovalent interactions, including base stacking, solvent-driven (hydrophobic) effects, and the geometric fit of aromatic nucleobases (*31*, *32*). Ethidium bromide and proflavine are the classic molecules for the investigation of intercalation (*33*). While much work has targeted the thermodynamics of binding of these intercalators, numerical values of the binding constants are disputed (*33*). Schelhorn and co-workers reported a binding constant of 3.5×10^4 M^{-1} for the intercalation of proflavine into DNA (*33*). Using the equation $\Delta G = -2.303\,RT \log K_{eq}$, a value of only −6.17 kcal/mol can be calculated for the energy associated with the binding of proflavine. One of the most potent DNA intercalators, 4-picoline-2,2′:6′,2″-terpyridine-platinum(II), has an equilibrium binding constant of 2×10^7 M^{-1} (*34*) or only −9.92 kcal/mol of binding energy. The addition of a small amount of energy for nitrogen inversion would not be sufficient to increase the stability difference between two conformers to a range where the two conformers could be detected.

The more plausible explanation is that of two different adducts, a C^{4a} and a N^5 adduct, in which the C^{4a} adduct decomposes but the N^5 adduct does not. If this occurs, the ratio for the two initial LC peaks (assigned to the adduct) to unmodified FAD and FMN should decrease by a factor of 3 (one adduct decomposes to FAD). If two conformers are interconverting, the ratio of adduct to flavin should remain constant. A rough determination of the area under the initial extracted mass peaks of 920 (Figure 9; two initial adduct peaks) compared with that for the combined FAD and FMN peaks, and the area under the final extracted mass peak of 920 (Figure 12; one final adduct peak) compared with the combined FAD and FMN peaks, shows the expected 3:1 ratio. These results support the model of two adducts forming initially (C^{4a} and N^5), but one, presumably the C^{4a}, decaying faster than the other (Scheme 2). Further support for this explanation comes from the observation that benzyl 1-aminomethylcyclopropanecarboxylate and *N*-cyclopropyl-1-methylbenzylamine inactivate MAO N with the spectra of a C^{4a} adduct; however, upon treatment of the adducts with acid, they decompose to unmodified FAD (data not shown).

CONCLUSION

UV−vis spectral data indicate the formation of an N^5 flavin adduct upon inactivation of MAO N by 1-PCPA. LC/ESI-MS results suggest that two flavin adducts are formed initially, but one decomposes faster than the other over time. The structure proposed for the flavin−1-PCPA adduct (Figure 6) is consistent with the mechanism in Scheme 1. Given the similarity of MAO N to MAO B, it is likely that the same mechanism is responsible for the formation of the flavin adduct with both enzymes. The similarity of the modified flavin structures resulting from both MAO B and MAO N with 1-PCPA would further support the ancestral relationship between these two flavoenzymes. Similar studies with MAO B are underway.

ACKNOWLEDGMENT

We thank Dr. Boyu Zhong for the generous gift of 1-PCPA and [2,3-$^{13}C_2$]-1-PCPA. We also thank the Analytical Services Laboratory at Northwestern University for support, as well as Klass Hallenga of the Cancer NMR Facility at the University of Chicago and Krish Krishnamurthy of Varian, Inc., for helpful discussions on the subject of nanomole scale NMR. D.J.M. carried out all enzyme inactivation and adduct isolation experiments. LC/ESI-MS work was carried out in collaboration with D.N. and R.B.v.B.; NMR spectroscopy was in collaboration with E.R. S.O.S. carried out the growth and purification of the MAO N enzyme. S.C. did the molecular modeling.

REFERENCES

1. Kohn, H. I. (1937) *Biochem. J. 31*, 1693−1704.
2. Singer, T. P., and Ramsay, R. R. (1995) *FASEB J. 9*, 605−610.
3. Knoll, J. (1992) *Med. Res. Rev. 12*, 505−524.
4. Robinson, D. S. (1989) in *Enzymes as Targets for Drug Design* (Palfreyman, M. G., McCann, P. P., Lovenberg, W., Temple, J. G., and Sjoerdsma, A., Eds.) p 233, Academic Press, San Diego.
5. Silverman, R. B. (1995) *Prog. Brain Res. 106*, 23−31.
6. Bach, A. W. J., Lan, N. C., Johnson, D. L., Abell, C. W., Bembenck, M. E., Kwan, S.-W., Seeburg, P. H., and Shih, J. C. (1988) *Proc. Natl. Acad. Sci. U.S.A. 85*, 4934−4938.
7. Bradford, M. M. (1976) *Anal. Biochem. 72*, 248−254.
8. Erwin, V. G., and Hellerman, L. (1967) *J. Biol. Chem. 242*, 4230−4238.
9. Schilling, B., and Lerch, K. (1995) *Biochim. Biophys. Acta 1243*, 529−537.
10. Schilling, B., and Lerch, K. (1995) *Mol. Gen. Genet. 247*, 430−438.
11. Sablin, S. O., Yankovskaya, V., Bernard, S., Cronin, C. N., and Singer, T. P. (1998) *Eur. J. Biochem. 253*, 270−279.
12. Paech, C., Salach, J. I., and Singer, T. P. (1980) *J. Biol. Chem. 255*, 2700−2704.
13. Silverman, R. B. (1983) *J. Biol. Chem. 258*, 14766−14769.
14. Silverman, R. B., and Zieske, P. A. (1985) *Biochemistry 24*, 2128−2138.
15. Silverman, R. B., and Zieske, P. A. (1986) *Biochem. Biophys. Res. Commun. 135*, 154−159.
16. Silverman, R. B., Cesarone, J. M., and Lu, X. (1993) *J. Am. Chem. Soc. 115*, 4955−4961.
17. Nagy, J., Kenney, W. C., and Singer, T. P. (1979) *J. Biol. Chem. 254*, 2684−2688.
18. Maycock, A. L., Abeles, R. H., Salach, J. I., and Singer, T. P. (1976) *Biochemistry 15*, 114−125.
19. McCann, A. E., and Sampson, N. S. (2000) *J. Am. Chem. Soc. 122*, 35−39.
20. Zhong, B., and Silverman, R. B. (1997) *J. Am. Chem. Soc. 119*, 6690−6691.
21. Zhong, B. (1998) Ph.D. Dissertation, Northwestern University.
22. Bradford, M. M. (1976) *Anal. Biochem. 72*, 248−254.
23. Summers, M. F., Marzilli, L. G., and Bax, A. (1986) *J. Am. Chem. Soc. 108*, 4285−4294.
24. Ghisla, S., Hartmann, U., Hemmerich, P., and Muller, F. (1973) *Liebigs Ann. Chem.*, 1388−1415.
25. Kellogg, R. M., Kruizinga, W., Bystrykh, L. V., Dijkhuizen, L., and Harder, W. (1992) *Tetrahedron 48*, 4147−4162.
26. Kyte, J. (1995) *Mechanism in Protein Chemistry*, Garland, New York.
27. Moonen, C. T. W., Vervoort, J., and Müller, F. (1984) *Biochemistry 23*, 4868−4872.
28. Moonen, C. T. W., Vervoort, J., and Müller, F. (1984) *Biochemistry 23*, 4859−4867.

29. Tauscher, L., Ghisla, S., and Hemmerich, P. (1973) *Helv. Chim. Acta 56*, 630−644.
30. Zheng, Y.-J., and Ornstein, R. L. (1996) *J. Am. Chem. Soc. 118*, 9402−9408.
31. Chupp, J. P., and Olin, J. F. (1967) *J. Org. Chem. 32*, 2297−2303.
32. Guckian, K. M., Schweitzer, B. A., Ren, R. X.-F., Sheils, C. J., Tahmassebi, D. C., and Kool, E. T. (2000) *J. Am. Chem. Soc. 122*, 2213−2222.
33. Matray, T. J., and Kool, E. T. (1998) *J. Am. Chem. Soc. 120*, 6191−6192.
34. Schelhorn, T., Kretz, S., and Zimmermann, H. W. (1992) *Cell. Mol. Biol. 38*, 345−365.
35. McCoubrey, A., Latham, H. C., Cook, P. R., Rodger, A., and Lowe, G. (1996) *FEBS Lett. 380*, 73−78.

BI010388Q